Genomics

Molecular Cancer Research

Expression of *ANRIL*–Polycomb Complexes–*CDKN2A/B/ARF* Genes in Breast Tumors: Identification of a Two-Gene (*EZH2/CBX7*) Signature with Independent Prognostic Value

Didier Meseure[1,2], Sophie Vacher[1], Kinan Drak Alsibai[2], Andre Nicolas[2], Walid Chemlali[1], Martial Caly[3], Rosette Lidereau[1], Eric Pasmant[4], Celine Callens[1], and Ivan Bieche[1,4]

Abstract

ANRIL, a long noncoding RNA (lncRNA), has recently been reported to have a direct role in recruiting polycomb repressive complexes PRC2 and PRC1 to regulate the expression of the p15/CDKN2B-p16/CDKN2A-p14/ARF gene cluster. Expression analysis of *ANRIL*, *EZH2*, *SUZ12*, *EED*, *JARID2*, *CBX7*, *BMI1*, *p16*, *p15*, and *p14/ARF* genes was evaluated in a large cohort of invasive breast carcinomas (IBC, $n = 456$) by qRT-PCR and immunohistochemistry (IHC) was performed on CBX7, EZH2, p14, p15, p16, H3K27me3, and H3K27ac. We observed significant overexpression in IBCs of *ANRIL* (19.7%) and *EZH2* (77.0%) and an underexpression of *CBX7* (39.7%). Correlations were identified between these genes, their expression patterns, and several classical clinical and pathologic parameters, molecular subtypes, and patient outcomes, as well as with proliferation, epithelial–mesenchymal transition, and breast cancer stem cell markers. Multivariate analysis revealed that combined *EZH2*/*CBX7* status is an independent prognostic factor ($P = 0.001$). In addition, several miRNAs negatively associated with *CBX7* underexpression and *EZH2* overexpression. These data demonstrate a complex pattern of interactions between lncRNA *ANRIL*, several miRNAs, PRC2/PRC1 subunits, and *p15/CDKN2B-p16/CDKN2A-p14/ARF* locus and suggest that their expression should be considered together to evaluate antitumoral drugs, in particular the BET bromodomain inhibitors.

Implications: This study suggests that the global pattern of expression rather than expression of individual family members should be taken into account when defining functionality of repressive Polycomb complexes and therapeutic targeting potential. *Mol Cancer Res; 14(7); 623–33. ©2016 AACR.*

Introduction

Invasive breast carcinomas (IBC) are highly heterogeneous tumors, and triple-negative subtype (TNC) remains a major cause of death in women. Although more than 90% of breast tumors are clinically localized, about 50% of them relapse within 5 years. Thus, identification of new prognostic factors and potential targeted therapies is crucial to improve outcome of patients with IBC.

Changes in the epigenetic landscape, including histone modifications, DNA methylation, and noncoding RNAs (ncRNA,) altered expression are now considered as a new hallmark of cancer (1). Polycomb repressive complexes (PRC) play important roles in chromatin remodeling and inhibition of transcription, suppressor genes silencing, and interconnection with major signaling pathways (2). Polycomb group protein subunits are essential regulators of embryonic stem cell pluripotency and early developmental cell fate decisions that are often deregulated in cancer. Two multiprotein complexes, PRC2 and PRC1, act concertedly and sequentially in transcriptional repression *via* two distinct histone modifications, trimethylation of lysine 27 on histone H3 (H3K27me3) and monoubiquitination of histone H2A (H2AK119ub). PRC2 contains mainly four subunits (EZH2, SUZ12, EED, and JARID2) and is involved in initiation of silencing by catalyzing methylation of histone H3 (3). PRC1 also comprises mainly four subunits (BMI1, PHC, CBX7, and RING1) and is implicated in maintenance of silencing by catalyzing monoubiquitination of histone H2A (ref. 4; Supplementary Fig. S1).

PRC2 and PRC1 have been described to interact with long noncoding RNAs (lncRNA). LncRNAs are defined by a length ranged from 200 bp to 100 kbp and their number is in constant increase: 48,680 lncRNAs are at present identified (5–7). LncRNAs are important regulators coordinating expression of protein-coding genes nearby (*cis*-regulation) or at distance (*trans*-regulation). LncRNAs function as guide, tethers, scaffolds, and decoys and their mechanisms of action are located at epigenetics, translational, and posttranslational levels (8). Accumulating data suggest that deregulation of lncRNAs is

[1]Unit of Pharmacogenomics, Department of Genetics, Curie Institute, Paris, France. [2]Platform of Investigative Pathology, Curie Institute, Paris, France. [3]Department of Biopathology, Curie Institute, Paris, France. [4]Faculty of Pharmaceutical and Biological Sciences, Paris Descartes University, Paris, France.

Note: Supplementary data for this article are available at Molecular Cancer Research Online (http://mcr.aacrjournals.org/).

Corresponding Author: Ivan Bieche, Unit of Pharmacogenomics, Department of Genetics, Institut Curie, 26 rue d'Ulm, Paris 75005, France. Phone: 331-7238-9363. Fax: 331-5310-2665; E-mail: ivan.bieche@curie.fr

doi: 10.1158/1541-7786.MCR-15-0418

pivotal in cancer initiation, progression, and metastatic spread. Among important lncRNAs deregulated in cancer, *ANRIL* (antisense noncoding RNA in the *INK4* locus) is encoded in the chromosome 9p21 region (9) and has been reported to have a direct role in recruiting PRC2 and PRC1 complexes to specific loci and in repressing gene expression (10). *ANRIL* is transcribed as a 3.8-kb lncRNA in the opposite direction from the *p15/CDKN2B-p16/CDKN2A-p14/ARF* gene cluster. Common disease genome-wide association studies (GWAS) have identified the *ANRIL* gene as a shared genetic susceptibility locus to coronary disease, intracranial aneurysm, type 2 diabetes, and numerous cancers (11). Increased *ANRIL* expression levels were observed in prostate carcinomas and involved in repression of the *CDKN2B/CDKN2A/ARF* gene cluster in *cis* by directly binding to PRC complexes (10). EZH2 (PRC2) and CBX7 (PRC1) act as transcriptional repressors of many genes and are particularly implicated in silencing *via ANRIL* of the *CDKN2B/CDKN2A/ARF* locus (12). However, the functional role and underlying mechanism of action of *ANRIL* in breast carcinogenesis still remain unclear (13).

The aim of the present study was to analyze at RNA and protein levels, the ribonucleoproteic network composed of the lncRNA *ANRIL*, the two polycomb complexes PRC2/PRC1, and the downstream *CDKN2B/CDKN2A/ARF* gene cluster, as well as several miRNAs targeting PRC units, in IBCs and to evaluate their clinical significance.

Materials and Methods

Patients and samples

Samples of 456 primary unilateral invasive primary breast tumors excised from women managed at Institut Curie (Saint-Cloud, France) from 1978 to 2008 have been analyzed. All patients cared in our institution before 2007 were informed that their tumor samples might be used for scientific purposes and had the opportunity to decline. Since 2007, patients treated in our institution have given their approval by signed informed consent. This study was approved by the local ethics committee (Breast Group of Rene Huguenin Hospital). Samples were immediately stored in liquid nitrogen until RNA extraction. A tumor sample was considered suitable for this study if the proportion of tumor cells exceeded 70%. The patients (mean age, 61.7 years; range, 31–91 years) all met the following criteria: primary unilateral nonmetastatic breast carcinoma for which complete clinical, histologic, and biologic data were available; no radiotherapy or chemotherapy before surgery; and full follow-up at Institut Curie. Treatment consisted of modified radical mastectomy in 283 cases (63.9%) and breast-conserving surgery plus locoregional radiotherapy in 160 cases (36.1%). The patients had a physical examination and routine chest radiography every 3 months for 2 years and then annually. Mammograms were done annually. Adjuvant therapy was administered to 369 patients, consisting of chemotherapy alone in 91 cases, hormone therapy alone in 176 cases, and both treatments in 102 cases. The histologic type and the number of positive axillary nodes were established at the time of surgery. The malignancy of infiltrating carcinomas was scored according to Scarff Bloom Richardson (SBR) histoprognostic system. Estrogen receptor (ERα), progesterone receptor (PR), and human EGF receptor 2 (ERBB2) status was determined at the protein level by using biochemical methods [dextran-coated charcoal method, enzyme immunoassay, or immunohistochemistry (IHC)] and confirmed by real-time quantitative RT-PCR assays (14, 15). The population was divided into 4 groups according to HR (*ERα* and *PR*) and *ERBB2* status, as follows: two luminal subtypes [HR+ (ERα+ or PR+)/ERBB2+ ($n = 54$)] and [HR+ (ERα+ or PR+)/ERBB2− ($n = 290$)]; an ERBB2+ subtype [HR− (ERα− and PR−)/ERBB2+ ($n = 45$)]; and a triple-negative subtype [HR− (ERα− and PR−)/ERBB2− ($n = 69$)]. Standard prognostic factors are shown in Supplementary Table S1. Patients ($n = 169$) developed metastasis during a median follow-up of 8.9 years (range, 6 months to 29 years). Ten specimens of adjacent normal breast tissue from patients with breast cancer ($n = 7$) and normal breast tissue from women undergoing cosmetic breast surgery ($n = 3$) were used as sources of normal RNA.

RNA extraction

Total RNA was extracted from breast tumor samples by using acid-phenol guanidium as previously described (16). RNA quality was determined by electrophoresis through agarose gels, staining with ethidium bromide, and visualization of the 18S and 28S RNA bands under ultraviolet light.

Real-time RT-PCR

LncRNA and protein-coding genes expression analysis. *ANRIL*, *EZH2*, *SUZ12*, *EED*, *JARID2*, *CBX7*, *BMI1*, *P16/CDKN2A*, *P15/CDKN2B*, and *P14/ARF* gene mRNA expression levels were quantified by using real time RT-PCR in a retrospective series of 456 well-characterized tumors. Quantitative values were obtained from the cycle number (C_t value) at which the increase in the fluorescence signal associated with exponential growth of PCR products started to be detected by the laser detector of the ABI Prism 7900 Sequence Detection System (Perkin-Elmer Applied Biosystems), using PE Biosystems analysis software according to the manufacturer's manuals. The precise amount of total RNA added to each reaction mix (based on optical density) and its quality (i.e., lack of extensive degradation) are both difficult to assess. We therefore also quantified transcripts of the *TBP* gene (Genbank accession: NM_003194) encoding the TATA box–binding protein (a component of the DNA-binding protein complex TFIID) as an endogenous RNA control and normalized each sample on the basis of its *TBP* content. We selected *TBP* as an endogenous control because the prevalence of its transcripts is moderate and because there are no known TBP retropseudogenes (retropseudogenes lead to coamplification of contaminating genomic DNA and thus interfere with RT-PCR, despite the use of primers in separate exons; ref. 14). Results, expressed as *N*-fold differences in target gene expression relative to the *TBP* gene and termed "N_{target}," were determined as $N_{target} = 2^{\Delta Ct\_sample}$, where the ΔC_t value of the sample was determined by subtracting the average C_t value of the target gene from the average C_t value of the *TBP* gene. The N_{target} values of the samples were subsequently normalized such that the median of the N_{target} values for the 10 normal breast tissues was 1. The primers for *TBP*, *ANRIL*, and the 9 protein-coding genes were chosen with the assistance of the Oligo 6.0 program (National Biosciences). We scanned the dbEST and nr databases to confirm the total gene specificity of the nucleotide sequences chosen for the primers and the absence of SNPs. To avoid amplification of contaminating gDNA, 1 of the 2 primers was placed at the junction between 2 exons or on 2 different exons. Agarose gel electrophoresis was used to verify the specificity of PCR amplicons. The conditions of cDNA synthesis and PCR were as described (17).

miRNAs expression analysis. miRNAs were isolated with the RNA extraction procedure used for the protein-coding transcripts (total RNA extraction). Reverse transcription was performed with the QIAGEN miScript Reverse Transcription Kit, according to the manufacturer's protocol (QIAGEN, GmbH). Specific miRNAs were quantified by real-time PCR with the QIAGEN miScript SYBR Green PCR Kit (QIAGEN). The small nucleolar RNU44 was used as an internal control. The relative expression level of each miRNA, expressed as *N*-fold difference in target miRNA expression relative to RNU44, and termed "N_{target}", was calculated as follows: $N_{target} = 2^{\Delta Ct\_sample}$. The ΔC_t value of a given sample was determined by subtracting the C_t value of the target miRNA from the C_t value of RNU44. The N_{target} values of the samples were subsequently normalized so that the median N_{target} value of samples with low level of *EZH2* and *CBX7* transcripts was 1.

IHC

We performed IHC assay by using CBX7 (Novus, polyclonal, rabbit, NBP1-79042, 1/250, pH6), EZH2 (Novocastra, monoclonal mouse, 6A10, 1/100, pH6), p15 (Abcam, polyclonal, rabbit, ab53034, 1/50, pH6), p16 (CINtec p16, Ventana 705-4713, mouse, monoclonal, E6H4 prediluted, 1 μg/mL), H3K27me2/3 [Abcam, anti-histone H3 (di- + tri-methyl K27), ab6147, mouse, monoclonal, 1/200, pH6], and H3K27ac [Abcam, ab 4729, Rabbit polyclonal to Histone H3 (acetyl K27), 1/400, pH6] antibodies in a series of 80 IBCs. Paraffin-embedded tissue blocks, obtained at the time of the initial diagnosis, were retrieved from the archives of the Department of Biopathology, Institut Curie. Sections of 3 μm were cut with a microtome from the paraffin-embedded tissue blocks of normal breast tissue, preinvasive lesions, and IBCs. Tissue sections were deparaffinized and rehydrated through a series of xylene and ethanol washes. Briefly, key figures included: (i) antigen retrieval in 0.1 mol/L citrate buffer, pH 6 (Biocare) in a pressure cooker (4 minutes); (ii) blocking of endogenous peroxidase activity by immersing sections in 3% hydrogen peroxide in methanol for 15 minutes and subsequently rinsing them in water and PBS; (iii) incubation with primary antibodies against the targeted antigen; (iv) immunodetection with a biotin-conjugated secondary antibody formulation that recognizes rabbit and mouse immunoglobulins, followed by peroxidase-labeled streptavidin and linking with a rabbit biotinylated antibody against mouse immunoglobulin G (DAKO SA); and (v) chromogenic revelation with AEC and counterstaining with Mayer's hematoxylin. All immunostaining was processed by using a DAKO automated immunostaining device. The specificity of the antibodies was confirmed by doing IHC studies with the same protocol on paraffin-embedded human tissue sections containing lymphocytes. A semiquantitative histologic score (*H*-score = intensity × frequency) was performed (score 0 = negative staining, score 1 = weak staining, score 2 = moderate staining, score 3 = strong staining).

Statistical analysis

The distributions of target mRNA levels were characterized by their median values and ranges. Relationships between mRNA levels of the different target genes and between mRNA (and protein) levels and clinical parameters were identified by using nonparametric tests, namely, the χ^2 test (relation between 2 qualitative parameters), the Mann–Whitney *U* test (relation between 1 qualitative and 1 quantitative parameter), and the Spearman rank correlation test (relation between 2 quantitative parameters). Differences were considered significant at confidence levels greater than 95% ($P < 0.05$). Metastasis-free survival (MFS) was determined as the interval between initial diagnosis and detection of the first metastasis. Survival distributions were estimated by the Kaplan–Meier method, and the significance of differences between survival rates was ascertained with the log-rank test. The Cox proportional hazards regression model was used to assess prognostic significance, and the results are presented as HRs and 95% confidence intervals (CI). Hierarchical clustering was performed with GenANOVA software (18).

Results

ANRIL and *EZH2* are upregulated, whereas *CBX7* is downregulated in IBCs

We measured mRNA levels of the lncRNA *ANRIL* and 6 genes belonging to the two repressive polycomb PRC2 and PRC1 complexes (PRC2: *EZH2*, *SUZ12*, *EED*, and *JARID2*; PRC1: *BMI1* and *CBX7*) in a series of 456 patients with unilateral invasive breast tumors and in a series of 10 normal breast tissues (including adjacent normal breast tissue from patients with breast cancer and normal breast tissue from women undergoing cosmetic breast surgery) by using quantitative RT-PCR assays (Table 1). We did not observe significant differences concerning the expression profiles of the 7 genes tested between the adjacent normal breast tissue from patients with breast cancer (7 samples) and normal breast tissue from women undergoing cosmetic breast surgery (3 patients; data not shown).The mRNA values of the breast cancer samples were normalized such that the median of the 10 normal breast tissue mRNA values was 1. To determine the cutoff point for altered target genes expression in breast cancer tissues, the N_{target} value, calculated as described in Materials and Methods, was determined for the 10 normal breast RNA samples. As these normal values were consistently between 0.39 (*CBX7*) and 2.45 (*ANRIL*), values of 0.33 or less were considered to represent underexpression, and values of 3 or more to represent overexpression of these genes in tumor samples. We have previously used the same approach to determine cutoff points for tumor gene altered expression (14, 19). In our series of 456 breast carcinomas, we observed overexpression of *ANRIL* in 19.7% of IBCs (median = 1.58; minimum = 0.05; maximum = 13.5). Concerning Polycomb subunits, we observed a marked overexpression of *EZH2* in 77.0% of IBCs (median = 5.09; minimum = 0.76; maximum = 48.3) and to a lesser extent of *BIM1* (median = 1.23; minimum = 0.00; maximum = 14.0) in 10.1% of IBCs and an unexpected underexpression of *CBX7* in 39.7% of IBCs (median = 0.38; minimum = 0.00; maximum = 2.59). *SUZ12*, *EED*, and *JARID2* were overexpressed only in 2.6%, 1.8%, and 5.1% of IBCs, respectively.

We performed an IHC analysis by using anti-EZH2 and anti-CBX7 antibodies in a series of 80 IBCs (standard prognostic factors are shown in Supplementary Table S2). We identified a moderate-to-intense nuclear staining of tumor cells (*H*-score = 2–3) with EZH2 antibodies in 75.9% of IBCs ($n = 63$ of 80) and an absence or a slight nuclear and cytoplasmic staining of tumor cells (*H*-score = 0–1) with CBX7 antibodies in 63.8% of IBCs ($n = 51$ of 80; Fig. 1).

The p15/CDKN2B-p16/CDKN2A-p14/ARF cluster is unexpectedly not silenced in IBCs

We measured mRNA levels of *p15/CDKN2B*, *p16/CDKN2A*, and *p14/ARF* in the series of 456 patients. We showed marked

Table 1. ANRIL pathway genes mRNA expression levels in the series of 456 breast tumors

Genes	Median C_t of normal breast tissue ($n = 10$)	Normal breast tissue ($n = 10$)	Breast tumors ($n = 456$)	Percentage of underexpressed tumors ($N_{target} < 0.33$)	Percentage of normal expressed tumors	Percentage of overexpressed tumors ($N_{target} > 3$)
ANRIL	34.07 (31.91–35.96)[a]	1.0 (0.35–2.45)[b]	1.58 (0.05–13.5)[b]	0.9[c]	79.4[c]	19.7[c]
Polycomb complex PRC2 genes ($n = 4$)						
EZH2	32.39 (31.23–34.30)	1.0 (0.48–2.32)	5.09 (0.76–48.3)	0	23.0	77.0
SUZ12	28.26 (27.17–29.98)	1.0 (0.56–1.25)	1.23 (0.43–59.2)	0	97.4	2.6
EED[d]	29.77 (28.70–33.16)	1.0 (0.58–1.84)	1.21 (0.03–7.74)	3.1	95.1	1.8
JARID2[e]	28.63 (27.3–30.55)	1.0 (0.83–1.46)	1.37 (0.34–8.53)	0	94.9	5.1
Polycomb complex PRC1 genes ($n = 2$)						
BMI1	28.40 (26.91–30.22)	1.0 (0.59–1.47)	1.23 (0.00–14.0)	4.2	85.8	10.1
CBX7	28.99 (27.78–31.25)	1.0 (0.39–1.62)	0.38 (0.00–2.59)	39.7	60.3	0
ANRIL regulated genes ($n = 3$)						
ARF	32.93 (31.69–34.75)	1.0 (0.21–2.41)	2.28 (0.00—105)	3.3	56.8	39.9
P16[f]	37.55 (34.64–50)	0.0 (0.0–6.95)	0.65 (0.0–63.4)	0	84.2	15.8
P15	30.89 (29.21–33.74)	1.0 (0.11–2.91)	1.62 (0.00–40.5)	7.0	71.3	21.7

[a]Median (range) of gene C_t values (cycle threshold).
[b]Median (range) of gene mRNA levels; the mRNA values of the samples were normalized such that the median of the 10 normal breast tissues mRNA values was 1.
[c]Percentage of underexpressing, normal, and overexpressing tumors using cutoffs of $N_{target} < 0.33$ and $N_{target} > 3$.
[d]Data available in 446 samples.
[e]Data available in 454 samples.
[f]The mRNA values of the samples were normalized such that a C_t value of 35 was 1.

overexpression of *p16*, *p14/ARF*, and *p15*, respectively, in 15.8%, 39.9%, and 21.7% of IBCs (Table 1).

We studied protein expression of p14, p16, and p15 in IBCs by using IHC in our series of 80 breast tumors. We observed nuclear and cytoplasmic overexpression of cancer cells (*H*-score = 2–3) with anti-p14, p16, and p15 antibodies in, respectively, 41.2% ($n = 33$ of 80), 51.3% ($n = 41$ of 80), and 37.5% ($n = 30$ of 80) of IBCs (Supplementary Fig. S2).

PRC2/PRC1 activity status revealed decrease of H3K27me3 expression levels and increase of H3K27ac expression levels in IBCs

To evaluate PRC2/PRC1 repressive activity status in breast tumors, we performed an IHC analysis in our series of 80 IBCs by using anti-H3K27me3 and anti-H3K27ac antibodies. We could identify an absence or a slight nuclear staining of cancer cells (*H*-score = 0–1) with H3K27me3 antibody in 76.3% of IBCs ($n = 61$ of 80) and a moderate-to-intense nuclear staining of tumor cells (*H*-score = 2–3) with H3K27ac antibody in 73.8% of IBCs ($n = 59$ of 80; Supplementary Fig. S3). An expected negative correlation was observed between staining of H3K27me3 and H3K27ac ($P = 0.0000073$).

ANRIL, PRC2/PRC1 subunits and *p15/CDKN2B-p16/CDKN2A-p14/ARF* cluster expression levels are associated with clinicopathologic parameters, molecular subtypes, and patient outcome

Clinicopathologic parameters. *ANRIL* mRNA expression level was exclusively and weakly correlated with ERα ($P = 0.038$) and PR ($P = 0.011$) status (Supplementary Table S3).

Concerning the PRC2 complex, *EZH2* mRNA expression level was strongly associated with SBR histologic grade ($P < 10^{-7}$), ERα status ($P = 3 \times 10^{-7}$), and PR status ($P = 3 \times 10^{-7}$), moderately associated with *ERBB2* status ($P = 0.00020$) and tumor size ($P = 0.0062$; Supplementary Table S4). Expression of *SUZ12* was exclusively associated with lymph node status ($P < 10^{-7}$; Supplementary Table S5), *EED* with SBR histologic grade ($P = 0.0011$), and PR status ($P = 0.0028$; Supplementary Table S6) and *JARID2* with ERα status ($P = 0.0027$) and ERBB2 status ($P = 0.0035$; Supplementary Table S7).

Concerning the PRC1 complex, *CBX7* mRNA expression level was highly significantly correlated with SBR histologic grade ($P = 0.000025$), ER status ($P = 0.000011$), and PR status ($P = 0.0000013$; Supplementary Table S8). *BMI1* was weakly associated with ERα status ($P = 0.036$) but not with any of other clinical predictive factors (Supplementary Table S9).

Finally, *ARF/p14* and *p16* mRNA expression levels were highly correlated with SBR histological grade ($P < 10^{-7}$ and $P = 0.000019$, respectively), ERα status ($P = 1.8 \times 10^{-7}$ and $P < 10^{-7}$, respectively), and PR status ($P = 1.3 \times 10^{-5}$ and $P = 1.8 \times 10^{-6}$, respectively; Supplementary Table S10), whereas *p15* was moderately correlated with ERα status ($P = 0.009$) and PR status ($P = 0.0008$), but not with SBR histologic grade, like *ARF/p14* and *p16* (Supplementary Tables S11 and S12).

It is also noteworthy that none of these 10 gene expressions showed significant link with the adjuvant treatment status including hormone therapy alone (176 patients), chemotherapy alone (91 patients), both hormone therapy and chemotherapy (102 patients), and no adjuvant therapy (87 patients; Supplementary Tables S3–S12).

Breast cancer molecular subtypes. By using HR (ERα and PR) and ERBB2 status, we subdivided our total population of IBCs ($n = 456$) into 4 subgroups: HR+/ERBB2+ ($n = 54$), HR+/ERBB2− ($n = 289$), HR−/ERBB2+ ($n = 45$), and HR−/ERBB2− ($n = 68$). *ANRIL*, PRC1/2 genes, and *p14/p15/p16* mRNA levels of expression in the different breast cancer molecular subtypes are shown in Supplementary Table S13. A strong correlation was observed between molecular subgroups and *ANRIL* ($P = 0.00013$), *EZH2* ($P < 10^{-7}$), *JARID2* ($P = 0.00090$), *CBX7* ($P = 0.000020$), and *p14/ARF* and *p16* ($P < 10^{-7}$) mRNA levels. High frequencies of *ANRIL*, *p14/ARF*, and *p16* deregulated expressions (under- or overexpressions) were mainly observed in triple-negative subtypes, *EZH2* overexpression, and *CBX7* underexpression in the two HR− subtypes, and *JARID2* overexpression in HR−/ERBB2+ subtypes (Supplementary Table S13).

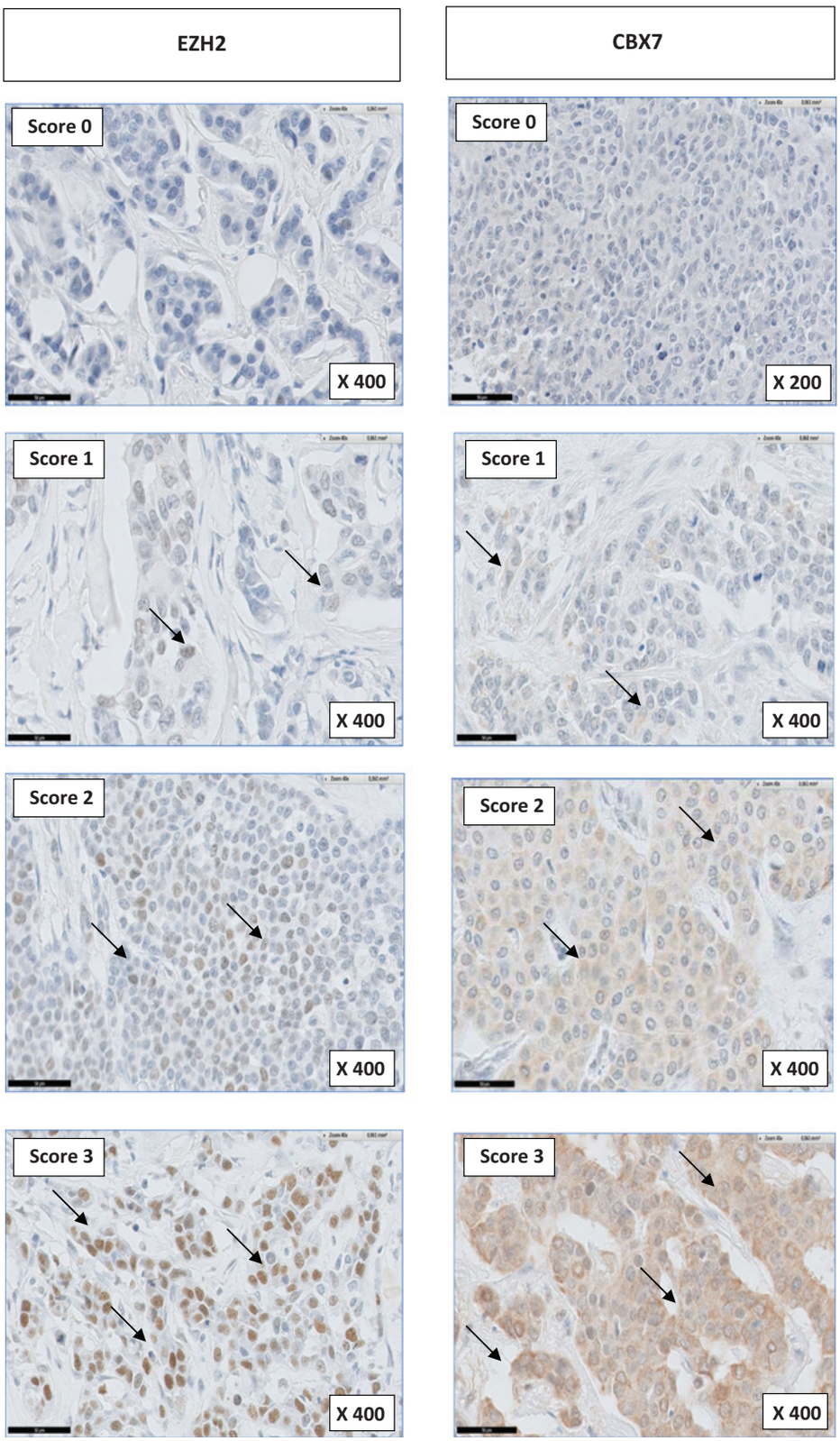

Figure 1.
IHC staining for EZH2 and CBX7. Nuclear overexpression of EZH2 (*H*-score = 2 and 3) in cancer cells was observed in 75.2% of IBCs and nuclear EZH2 underexpression in 24.8% of IBCs. Nuclear and cytoplasmic under expression of CBX7 (*H*-score = 0 and 1) was observed in 63.8% of IBCs and nuclear and cytoplasmic CBX7 overexpression in 36.2% of IBCs. Score 0, no cytoplasmic staining for CBX7 or nuclear staining for EZH2 is seen in tumor cells; Score 1, weak cytoplasmic staining for CBX72 and weak nuclear staining for EZH is seen in a subset of tumor cells; Score 2, moderate cytoplasmic staining for CBX7 and moderate nuclear staining for EZH2 is seen in a subset of tumor cells; Score 3: strong and diffuse cytoplasmic staining for CBX7, and strong nuclear staining for EZH2 is seen in most of tumor cells.

Table 2. Relationship between ANRIL pathway gene mRNA levels and MFS in the 456 breast tumors

Gene mRNA expression	Population (%)	Number of metastases (%)	P^a
Total population (%)	456 (100.0)	169 (37.1)	
ANRIL			
Non-overexpression	366 (80.3)	129 (76.3)	0.062 (NS)
Overexpression	90 (19.7)	40 (23.7)	
EZH2			
Non-overexpression	105 (23.0)	20 (11.8)	0.000045
Overexpression	351 (77.0)	149 (88.2)	
SUZ12			
Non-overexpression	444 (97.4)	163 (96.4)	0.71 (NS)
Overexpression	12 (2.6)	6 (3.6)	
EED[b]			
Underexpression	14 (3.1)	3 (1.8)	0.20 (NS)
Nonunderexpression	432 (96.9)	161 (98.2)	
JARID2[c]			
Non-overexpression	431 (94.9)	161 (96.4)	0.80 (NS)
Overexpression	23 (5.1)	6 (3.6)	
BMI			
Non-overexpression	410 (89.9)	148 (87.6)	0.49 (NS)
Overexpression	46 (10.1)	21 (12.4)	
CBX7			
Underexpression	181 (39.7)	79 (46.7)	0.0051
Non-underexpression	275 (60.3)	90 (53.3)	
ARF			
Non-overexpression	274 (60.1)	96 (56.8)	0.086 (NS)
Overexpression	182 (39.9)	73 (43.2)	
P16			
Normal expression	384 (84.2)	137 (81.1)	0.025
Overexpression	72 (15.8)	32 (18.9)	
P15			
Non-overexpression	357 (78.3)	128 (75.7)	0.090 (NS)
Overexpression	99 (21.7)	41 (24.3)	

Abbreviation: NS, not significant.
[a]Log-rank test.
[b]Information available for 446 patients.
[c]Information available for 454 patients.

Patient outcome. We assessed the impact of variations of *ANRIL*, *EZH2*, *SUZ12*, *EED*, *JARID2*, *CBX7*, *BMI1*, *p14/ARF*, *p15*, and *p16* mRNA levels on patient outcome. We used a log-rank test to identify relations between MFS and mRNA levels of these 10 genes (Table 2). *EZH2* overexpression and *CBX7* underexpression were significantly associated with shorter MFS ($P = 0.000045$ and $P = 0.0051$, respectively). We observed also a light significant difference in MFS among patients with *p16* overexpression ($P = 0.025$). MFS was not influenced by expression status of *ANRIL* and other genes analyzed (i.e. *SUZ12*, *EED*, *JARID2*,*BMI1*, *ARF*, and *p15*).

Two molecular markers may provide a more accurate prediction of patient outcome when combined than when considered in isolation. By combining *EZH2* and *CBX7* status, we identified four separate prognostic groups with significantly different MFS curves ($P = 0.00011$; Fig. 2). The patients with the poorest prognosis had *EZH2* overexpression and *CBX7* underexpression [5-year MFS: 61.7% (57.7%–65.7%); 10-year MFS: 51.4% (47.2%–55.6%)], whereas those with the best prognosis had *EZH2* and *CBX7* normal expression [5-year MFS: 86.4% (82.4%–90.4%); 10-year MFS: 81.2% (76.5%–85.9%)].

Multivariate analysis (Cox proportional hazards model) showed that lymph node status, tumor size, and combined *EZH2*/*CBX7* status were independent variables predictive of MFS ($P = 0.00021$, $P = 0.014$, and $P = 0.001$, respectively; Supplementary Table S14).

There is a complex interplay between *ANRIL, PRC1/PRC2 subunits* and *p15/CDKN2B-p16/CDKN2A-p14/ ARF* genes cluster

By using the Spearman rank correlation test for continuous variables, we could find a strong positive correlation between mRNA expression levels of the following genes belonging to the *ANRIL* pathway: (i) *ANRIL* and both *ARF* ($r = +0.594$, $P < 10^{-7}$), *p15* ($r = +0.381$, $P < 10^{-7}$), and *p16* ($r = +0.323$, $P < 10^{-7}$); (ii) *EZH2* and both *EED* ($r = +0.295$, $P < 10^{-7}$), *JARID2* ($r = +0.278$, $P < 10^{-7}$), and *BMI1* ($r = +0.229$, $P = 0.0000031$); and (iii) *SUZ12* and *CBX7* ($r = +0.317$, $P < 10^{-7}$), reflecting very complex interplay across this gene set (Supplementary Table S15).

Hierarchical clustering of *ANRIL* pathway genes according to their expression patterns in the series of 456 IBCs represented in dendrogram format, subdivided genes into two subgroups (Supplementary Fig. S4). Group I included *ANRIL*, *p14/ARF*, *p15*, *p16*, *EZH2*, *EED*, *JARID2*, and *BMI1* and contained 4 genes, *ANRIL* and the *p15/CDKN2B-p16/CDKN2A-p14/ARF* gene cluster, highly related. Group II included *SUZ12* (from the PRC2 complex) and *CBX7* (from the PRC1 complex).

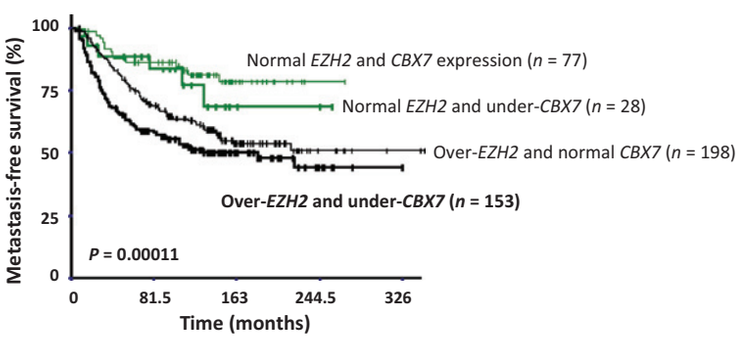

Patients at risk (*n*)				
Normal EZH2 and CBX7	59	15	2	0
Normal EZH2 and under-CBX7	17	4	2	0
Over-EZH2 and normal CBX7	114	37	10	3
Over-EZH2 and under-CBX7	78	27	8	1

Figure 2.
Survival curves of 4 patients groups according to EZH2 mRNA overexpression (over-EZH2) and CBX7 mRNA underexpression (under-CBX7) in the series of 456 breast tumors.

Table 3. Correlations between ANRIL pathway and EMT, proliferation and breast cancer stem cell genes mRNA expression levels in the series of 456 breast tumors

	EMT		Proliferation	Stem cell		
	VIM	***TWIST1***	***MKI67***	***ALDH1A1***	***ALDH1A3***[c]	***CD133***[d]
ANRIL	+0.134[a]	+0.117	+0.187	+0.182	+0.050	−0.098
	0.0043	0.012	0.0001	0.00015	0.29 (NS)	0.038
EZH2	−0.068	−0.010	+0.738	−0.164	+0.109	+0.043
	0.14 (NS)	0.83 (NS)	<0.0000001	0.00057	0.020	0.37 (NS)
SUZ12	+0.165	+0.131	+0.191	+0.049	+0.013	−0.128
	0.00052	0.0053	0.000075	0.30 (NS)	0.78 (NS)	0.0073
EED[b]	+0.115	+0.123	+0.208	+0.123	+0.295	+0.155
	0.014	0.0092	0.000023	0.0093	<0.0000001	0.0015
JARID2[c]	+0.214	+0.116	+0.276	+0.061	+0.233	+0.088
	0.000012	0.013	<0.0000001	0.19 (NS)	0.0000022	0.064 (NS)
BMI1	−0.141	−0.081	+0.176	−0.122	−0.071	−0.199
	0.0028	0.080 (NS)	0.00023	0.0087	0.13 (NS)	0.0000053
CBX7	+0.300	+0.328	−0.261	+0.464	+0.190	−0.028
	<0.0000001	<0.0000001	0.00000016	<0.0000001	0.000082	0.57 (NS)
ARF	−0.032	+0.059	+0.351	−0.029	+0.126	+0.043
	0.50 (NS)	0.20 (NS)	<0.0000001	0.54 (NS)	0.0071	0.37 (NS)
P16	+0.035	+0.154	+0.114	+0.001	+0.185	+0.160
	0.47 (NS)	0.0011	0.015	0.97 (NS)	0.00013	0.00093
P15	+0.155	+0.279	+0.025	+0.178	+0.282	+0.034
	0.0011	<0.0000001	0.60 (NS)	0.00021	<0.0000001	0.48 (NS)

Abbreviation: NS, not significant.
[a]Spearman rank correlation test.
[b]Data available in 446 samples.
[c]Data available in 454 samples.
[d]Data available in 438 samples.

Correlations of *ANRIL* and *PRC2/PRC1* genes expression levels with epithelial–mesenchymal transition, proliferation, and breast cancer stem cell markers

Data from the literature have suggested that Polycomb complexes are implicated in proliferation, epithelial–mesenchymal transition (EMT) induction, and stem cell differentiation. In consequence, we tested the possible links between *ANRIL* pathway gene expression and mRNA levels of various markers of proliferation (i.e., *MKI67*), of EMT (i.e., *VIM* and *TWIST1*), and of breast cancer stem cell (i.e., *ALDH1A1*, *ALDH1A3*, and *CD133*) in our series of 456 IBCs (Table 3). Marked positive associations were observed between *CBX7* and two EMT markers (*VIM* and *TWIST1*; $P < 10^{-7}$ and $P < 10^{-7}$, respectively). A significant positive correlation was also identified between *CBX7* and one breast cancer stem cell marker (*ALDH1A1*; $P < 10^{-7}$). *EZH2* was highly linked to MKI67 ($P < 10^{-7}$), whereas *EED* was linked to two breast cancer stem cell markers: *ALDH1A3* and *CD133* ($P < 10^{-7}$ and $P = 0.000082$, respectively).

As previous studies suggested a role of ANRIL in EMT (13), we further investigated the correlations between the expression levels of *ANRIL* and 9 different biomarkers of EMT in a series of 60 breast carcinomas (30 tumors with high expression level for ANRIL and 30 tumors with low expression level for *ANRIL*). We confirmed the absence of significant associations between *ANRIL* and various EMT-associated markers including *TWIST1*, *ZEB1*, *ZEB2*, *SNAI1/Snail*, *SNAI2/Slug*, *VIM/Vimentin*, *CDH2/N-cadherin*, *CDH1/E-cadherin*, and *ZO-1* (Supplementary Table S16).

miRNAs are implicated in posttranscriptional regulation of *PRC1/PRC2*

Previous studies suggested complex regulations between Polycomb subunit genes and miRNAs in carcinomas (20, 21). To investigate roles of miRNAs in posttranscriptional deregulation of the *ANRIL*/PRC pathway in IBCs, we selected 17 miRNAs from the literature. Among them, 4 miRNAs (miR-26A1, miR-101, miR-125B2, and miR-214) are known to target directly *EZH2* transcript (22–24) and 2 miRNAs (miR-181B1, miR-181A2) to target directly *CBX7* transcript (25). The 11 others miRNAs also target putatively *EZH2* and *CBX7* (26). We analyzed expression of these 17 miRNAs, using real-time quantitative RT-PCR, in IBCs with normal ($n = 20$) and marked low ($n = 20$) levels of *CBX7* transcripts and with normal ($n = 20$) and marked high ($n = 20$) levels of *EZH2* transcripts. We showed that (i) miR-181B1, miR-181A2, and miR-203 levels were marked significantly increased ($P < 0.01$) in *CBX7*-underexpressed tumors (Table 4) and that (ii) miR-26A1 and miR-125B1 levels were significantly decreased in *EZH2*-overexpressed tumors (Table 5).

These results of microRNA levels, shown in Tables 4 and 5, were standardized versus RNU44 as endogenous microRNA control. Similar results (significantly links between microRNA and *CBX7* and *EZH2* expressions) were obtained using a second well-known endogenous microRNA control (i.e., miR-191).

Discussion

Among the major discovered lncRNAs deregulated in carcinogenesis, *ANRIL* has been shown to regulate its neighbor tumor suppressor genes *CDKN2B*, *CDKN2A*, and *ARF* by epigenetic mechanisms and thereby control cell proliferation and senescence (27). *ANRIL*, acting in *cis*, specifically binds various Polycomb proteins, in particular EZH2 (PRC2) and CBX7 (PRC1), resulting in histone modification in the *CDKN2A/CDKN2B/ARF* locus. EZH2 is a histone methyltransferase and a member of PRC2 that not only methylates histone H3 on Lysine 27 but also interacts with and recruits DNA methyltransferases to methylate CpG of certain *EZH2* target genes to

Table 4. Statistical analysis of microRNAs expressions relative to CBX7 mRNA expression level

MiRNAs	Breast cancer with underexpression of CBX7 ($n = 20$)	Breast cancer with normal expression of CBX7 ($n = 20$)	P^a	ROC-AUC[b]
MIRN181B1	1.0 (0.22–2.29)[a]	0.34 (0.12–1.30)[b]	0.000024	0.11
MIRN181A2	1.0 (0.33–4.83)	0.39 (0.13–1.92)	0.00011	0.142
MIRN203	1.0 (0.25–4.72)	0.42 (0.16–1.02)	0.0058	0.245
MIRN200C	1.0 (0.22–3.34)	0.45 (0.11–1.77)	0.02	0.285
MIRN98	1.0 (0.17–7.66)	0.76 (0.14–3.35)	0.048	0.317
MIRN200B	1.0 (0.20–3.33)	0.73 (0.24–1.94)	0.11 (NS)	0.352
MIRN21	1.0 (0.25–3.62)	0.97 (0.13–6.49)	0.30 (NS)	0.405
MIRN192	1.0 (0.20–7.00)	0.75 (0.11–84.4)	0.37 (NS)	0.418
MIRN219-1	1.0 (0.00–4.05)	0.55 (0.10–7.50)	0.59 (NS)	0.45
MIRN200A	1.0 (0.02–3.92)	0.79 (0.14–6.33)	0.65 (NS)	0.458
MIRN183	1.0 (0.30–4.93)	0.55 (0.07–3.84)	0.70 (NS)	0.465
MIRN138-2	1.0 (0.09–33.9)	2.10 (0.06–41.0)	0.89 (NS)	0.512
MIRN217	1.0 (0.22–2.96)	1.32 (0.19–7.49)	0.23 (NS)	0.611
MIRN214	1.0 (0.29–2.12)	1.51 (0.26–3.22)	0.088 (NS)	0.658
MIRN101-1	1.0 (0.17–4.02)	1.95 (0.26–13.4)	0.041	0.689
MIRN125B1	1.0 (0.43–4.51)	2.12 (0.27–12.1)	0.019	0.718
MIRN26A1	1.0 (0.24–4.64)	3.05 (0.57–21.4)	0.015	0.725

Abbreviations: AUC, area under curve; NS, not significant; ROC, receiver operating characteristics.
[a]Kruskal–Wallis *H* test.
[b]Median (range) of microRNA levels.

establish firm repressive chromatin structures, contributing to tumor progression. CBX7 is a Chromobox family protein and a member of the PRC1 and is directly involved in regulation of genes frequently silenced in cancer.

To assess expression of the lncRNA *ANRIL* and the Polycomb subunits of *PRC2/PRC1* as well as *CDKN2A/CDKN2B/ARF* locus in IBCs, we used qRT-PCR in a large series of 456 IBCs from patients with known clinical and pathologic status and long-term outcome. Evaluation at mRNA level was combined with an IHC study in a series of 80 IBCs. Indeed, these two techniques of expression analysis (qRT-PCR and IHC) give complementary information, the technique of qRT-PCR with an extraction in homogeneous solution quantified transcripts levels both in tumor cells and in stroma cells, while IHC study allows only a semiquantitative analysis of protein levels, but on an individual cell basis (allowing distinction between epithelial tumor cells and stroma cells).

In the present study, we observed *ANRIL* overexpression in 19.7% of IBCs. *ANRIL* depletion has been associated with reduced proliferation (28), suggesting a procarcinogenic role supported by overexpression of this lncRNA in various others cancer types (29–31). In our IBC series, *ANRIL* overexpression was observed more particularly in the aggressive TNC subtype.

We also observed a marked overexpression of *EZH2* and to a lesser extent of *BMI1*, respectively, in 77.0% and 10.1% of IBCs and *CBX7* underexpression in 39.7% of the tumors. We confirmed these data at the protein level in the series of 80 IBCs by identifying a moderate and intense nuclear staining with an anti-EZH2 antibody in 82% of IBCs and an absence or a slight nuclear and cytoplasmic staining of cancer cells with a CBX7 antibody in 43%

Table 5. Statistical analysis of microRNAs expressions relative to EZH2 mRNA expression level

MicroRNAs	Breast cancer with normal expression of EZH2 ($n = 20$)	Breast cancer with overexpression of EZH2 ($n = 20$)	P^a	ROC-AUC
MIRN26A1	1.0 (0.17–6.46)[b]	0.29 (0.04–5.76)[b]	0.0027	0.222
MIRN125B1	1.0 (0.09–5.74)	0.37 (0.14–1.60)	0.0063	0.247
MIRN214	1.0 (0.11–2.35)	0.44 (0.20–1.42)	0.016	0.277
MIRN101-1	1.0 (0.06–7.72)	0.51 (0.13–1.99)	0.37 (NS)	0.417
MIRN217	1.0 (0.14–4.25)	0.45 (0.18–465)	0.69 (NS)	0.464
MIRN138-2	1.0 (0.12–36.3)	0.67 (0.07–25.7)	0.70 (NS)	0.465
MIRN192	1.0 (0.09–97.0)	0.91 (0.26–7.65)	0.85 (NS)	0.482
MIRN21	1.0 (0.08–3.86)	0.85 (0.21–5.98)	0.98 (NS)	0.498
MIRN203	1.0 (0.48–3.16)	1.59 (0.29–8.84)	0.76 (NS)	0.529
MIRN200A	1.0 (0.14–3.75)	1.66 (0.25–13.7)	0.30 (NS)	0.595
MIRN98	1.0 (0.43–3.47)	1.50 (0.26–13.2)	0.088 (NS)	0.657
MIRN200C	1.0 (0.45–2.37)	1.59 (0.28–8.50)	0.055 (NS)	0.677
MIRN200B	1.0 (0.17–1.77)	1.23 (0.40–8.87)	0.048	0.682
MIRN183	1.0 (0.05–4.35)	1.06 (0.26–10.8)	0.04	0.69
MIRN181A2	1.0 (0.20–2.28)	1.54 (0.46–5.97)	0.027	0.705
MIRN219-1	1.0 (0.16–3.56)	1.92 (0.32–14.0)	0.019	0.716
MIRN181B1	1.0 (0.41–2.37)	1.94 (0.44–5.30)	0.011	0.738

NOTE: miRNA levels were standardized versus U44 control microRNA.
Abbreviations: AUC, area under curve; NS, not significant; ROC, receiver operating characteristics.
[a]Kruskal–Wallis *H* test.
[b]Median (range) of microRNA levels.

of IBCs. In malignant tumors, *ANRIL* is a natural antisense transcript which usually recruits the two Polycomb repressor complexes PRC2 and PRC1, resulting in chromatin reorganization with silencing of the *INK4A/ARF/INK4B* locus. For example, positive links were observed between *CBX7* overexpression, *ANRIL* overexpression, and *CDKN2A/CDKNB/ARF* underexpression in prostate cancer (10). Conversely, in our series of breast tumors, we showed marked *CBX7* underexpression and a nonexpected high positive link between *ANRIL* overexpression and *CDKN2A/CDKNB/ARF* overexpression, and more particularly with *p14/ARF*. Although these results seem to be contradictory, it can be hypothesized that CBX7 can exhibit both oncosuppressive and oncogenic functions, depending on type of cancer, microenvironment, and presence of interacting proteins (32–35).

CBX7 underexpression was strongly correlated with high SBR histologic grade, negative ERα and PR status, and EMT and breast cancer stem cell markers. Apart from few exceptions (as prostate cancer), CBX7 expression is lost in human malignant neoplasias, and a clear correlation between its downregulated expression and a cancer aggressiveness and poor prognosis has been observed (36).

EZH2 overexpression was also strongly associated with high SBR histologic grade and negative ERα and PR status. But, unlike *CBX7*, *EZH2* overexpression was highly linked to the proliferation marker *MKI67*, suggesting a different role of these two proteins in breast tumorigenesis (37). Numerous studies point on the widespread roles of PRC2 (as well as H3K27 methylation) in developmental and differentiation processes of multicellular organisms, and on their implication in fundamental chromatin mechanisms that underlie stem cell regulatory circuits and cancer progression (38). Thus, it is not surprising that increasing evidences indicate that EZH2 deregulation is frequently observed in a variety of cancers (39–41). EZH2 overexpression is mainly found in solid tumors (as in our present study in breast cancer), whereas activating or inactivating mutations are identified in hematologic malignancies (42).

Using log-rank analysis to identify relations between MFS and mRNA levels of the 10 *ANRIL* pathway genes, only *EZH2* overexpression and *CBX7* underexpression were significantly associated with shorter MFS. Multivariate analysis showed that combined *EZH2/CBX7* status was an independent prognostic factor.

Results from previous studies suggest complex interactions between Polycomb complexes and miRNAs in cancer progression. As no mutation or allelic loss of *CBX7* located in 22q13.1 were identified in large genomic studies (43) and focal amplification of *EZH2* located in 7q36 was only observed in 1% of IBCs (43), we suspected epigenetic mechanisms implicating miRNAs could account for *CBX7* underexpression and *EZH2* overexpression in IBCs. Among the 17 miRNAs selected, (i) miR-181B1, miR-181A2, and miR-203 expressions were significantly increased in IBCs with *CBX7* underexpression and (ii) miR-26A1 and miR-125B2 expressions were significantly decreased in IBCs with *EZH2* overexpression, in agreement with the literature (44, 45). Our results thus showed that *EZH2* is targeted by 3 oncosuppressive miRNAs (miR-26A1, miR-125B, and miR-214) that are decreased in IBCs, suggesting an epigenetic mechanism of *EZH2* overexpression in IBCs. Concerning *CBX7*, our results were also consistent with recent data in the literature, suggesting that the 2 oncomiRs miR-181B1 and miR-181A2 could be induced by the oncogene *HMGA1*, resulting in *CBX7* underexpression (46). Indeed, we observed a positive link between *HMGA1* mRNA levels and expression of both miR-181B1 ($r = +0.340$, $P = 0.0038$) and miR-181A2 ($r = +0.264$, $P = 0.025$) in 71 tumors of our IBC series (data not shown).

Recent data revealed that histone modifier complexes PRC2 and PRC1 have a bivalent role in cancer, bearing both oncogenic and tumor-suppressive properties depending on cell tumor type (47). Complex deficiency in PRC2 and PRC1 components could decrease expression levels of epigenetic repressive mark H3K27 trimethylation, thereby contributing to H3K27 acetylation and resulting in increased transcription and activation of oncogenic pathways. Thus, defining a PRC2/PRC1 activity status in IBCs may be pivotal in combining or reconsidering therapeutic options. We identified a moderate-to-intense nuclear staining of tumor cells with H3K27ac antibodies in 73.8% of IBCs associated to an absence or a slight nuclear staining of cancer cells with H3K27me3 antibody in 76.3% of IBCs. Collectively, these data suggest that loss of Polycomb repressive function in IBCs might be due to epigenetic alteration of PRC1 and PRC2 by several microRNA targeting CBX7 and EZH2, resulting in altered H3K27trimethylation and H3K27 acetylation. Development of therapies targeting epigenetic processes in cancer has gained increasing focus with study of HDAC and DNA methyltransferase inhibitors and more recently of BET bromodomain inhibitors (48). Indeed, recent studies of malignant peripheral nerve sheath tumors (MPNST) have showed that alterations of PRC2 subunits lead to the amplification of Ras-driven transcription and confer sensitivity to BET bromodomain inhibitors (49, 50).

In conclusion, our results revealed a complex pattern of interactions between *ANRIL*, PRC2/PRC1 and suppressive and oncogenic miRNAs in IBCs. Our findings also point to *EZH2* and *CBX7* as the most promising of the 10 genes investigated for clinical applications and therapeutic approaches to breast cancer. This study suggest that it is the global pattern of expression, rather than expression of individual family members, that should be taken into account when defining functionality of repressive Polycomb complexes and evaluating antitumor drugs targeting these genes. Thus, establishment of a PRC2/PRC1 activity status in IBCs could be contributive in targeting BET proteins by using bromodomain inhibitors when levels of H3K27me3 are decreased and H3K27ac increased. Moreover, inhibition of oncomiRNAs miR-181B1 and miR-181A2 (as well as restoration of oncosuppressive miR-26A1, miR-125B, and miR-214) may represent another attractive combined strategy for breast cancer–targeted therapy.

Disclosure of Potential Conflicts of Interest

No potential conflicts of interest were disclosed.

Authors' Contributions

Conception and design: D. Meseure, E. Pasmant, I. Bieche

Development of methodology: D. Meseure, S. Vacher, I. Bieche

Acquisition of data (provided animals, acquired and managed patients, provided facilities, etc.): D. Meseure, S. Vacher, K. Drak Alsibai, A. Nicolas, I. Bieche

Analysis and interpretation of data (e.g., statistical analysis, biostatistics, computational analysis): D. Meseure, S. Vacher, K. Drak Alsibai, W. Chemlali, R. Lidereau, I. Bieche

Writing, review, and/or revision of the manuscript: D. Meseure, E. Pasmant, C. Callens, I. Bieche
Administrative, technical, or material support (i.e., reporting or organizing data, constructing databases): K. Drak Alsibai, M. Caly, C. Callens, I. Bieche
Study supervision: I. Bieche

Grant Support

This work was supported by grant INCa-DGOS-4654.

The costs of publication of this article were defrayed in part by the payment of page charges. This article must therefore be hereby marked *advertisement* in accordance with 18 U.S.C. Section 1734 solely to indicate this fact.

Received October 15, 2015; revised March 23, 2016; accepted April 8, 2016; published OnlineFirst April 21, 2016.

References

1. Piao HL, Ma LJ. Non-coding RNAs as regulators of mammary development and breast cancer. J Mammary Gland Biol Neoplasia 2012;17:33–42.
2. Kerppola TK. Polycomb group complexes: many combinations, many functions. Trends Cell Biol 2009;19:692–704.
3. Margueron R, Reinberg D. The Polycomb complex PRC2 and its mark in life. Nature 2011;469:343–9.
4. Luis NM, Morey L, Di Croce L, Benitah SA. Polycomb in stem cells: PRC1 branches out. Cell Stem Cell 2012;11:16–21.
5. Iyer MK, Niknafs YS, Malik R, Singhal U, Sahu A, Hosono Y, et al. The landscape of long noncoding RNAs in the human transcriptome. Nat Genet 2015;47:199–208.
6. Derrien T, Johnson R, Bussotti G, Tanzer A, Djebali S, Tilgner H, et al. The GENCODE v7 catalog of human long noncoding RNAs: analysis of their gene structure, evolution, and expression. Genome Res 2012; 22:1775–89.
7. Harrow J, Frankish A, Gonzalez JM, Tapanari E, Diekhans M, Kokocinski F, et al. GENCODE: the reference human genome annotation for The ENCODE Project. Genome Res 2012;22:1760–1774.
8. Wang KC, Chang HY. Molecular mechanisms of long noncoding RNAs. Mol Cell 2011;43:904–14.
9. Pasmant E, Laurendeau I, Héron D, Vidaud M, Vidaud D, Bièche I. Characterization of a germ-line deletion, including the entire INK4/ARF locus, in a melanoma-neural system tumor family: identification of ANRIL, an antisense noncoding RNA whose expression coclusters with ARF. Cancer Res 2007;67:3963–9.
10. Yap KL, Li S, Munoz-Cabello AM, Raguz S, Zeng L, Mujtaba S, et al. Molecular interplay of the noncoding RNA ANRIL and methylated histone H3 lysine 27 by polycomb CBX7 in transcriptional silencing of INK4a. Mol Cell 2010;38:662–74.
11. Pasmant E, Sabbagh A, Masliah-Planchon J, Ortonne N, Laurendeau I, Melin L, et al. Role of noncoding RNA ANRIL in genesis of plexiform neurofibromas in neurofibromatosis type 1. J Natl Cancer Inst 2011; 103:1713–22.
12. Popov N, Gil J. Epigenetic regulation of the INK4b-ARF-INK4a locus: in sickness and in health. Epigenetics 2010;5:685–90.
13. Li CH, Chen Y. Targeting long non-coding RNAs in cancers: progress and prospects. Int J Biochem Cell Biol 2013;45:1895–910.
14. Bieche I, Onody P, Laurendeau I, Olivi M,Vidaud D, Lidereau R, et al. Real-time reverse transcription-PCR assay for future management of ERBB2-based clinical applications. ClinChem 1999;45:1148–56.
15. Bieche I, Parfait B, Laurendeau I, Girault I, Vidaud M, Lidereau R. Quantification of estrogen receptor alpha and beta expression in sporadic breast cancer. Oncogene 2001;20:8109–15.
16. Chomczynski P, Sacchi N. Single-step method of RNA isolation by acid guanidiniumthiocyanate-phenol-chloroform extraction. Anal Biochem 1987;162:156–9.
17. Bieche I, Parfait B, Le Doussal V, Olivi M, Rio MC, Lidereau R, et al. Identification of CGA as a novel estrogen receptor-responsive gene in breast cancer: an outstanding candidate marker to predict the response to endocrine therapy. Cancer Res 2001;61:1652–8
18. Didier G, Brezellec P, Remy E, Henaut A. GeneANOVA-gene expression analysis of variance. Bioinformatics 2002;18:490–1.
19. Bieche I, Noguès C, Lidereau R. Overexpression of BRCA2 gene in sporadic breast tumours. Oncogene 1999;18:5232–8.
20. Cao Q, Mani RS, Ateeq B, Dhanasekaran SM, Asangani IA, Prensner JR, et al. Coordinated regulation of polycomb group complexes through microRNAs in Cancer. Cancer Cell 2011;20:187–99.
21. Ye S, Yang L, Zhao X, Song W, Wang W, Zheng S. Bioinformatics method to predict two regulation mechanism: TF-miRNA-mRNA and lncRNA-miRNA-mRNA in pancreatic cancer. Cell Biochem Biophys 2014;5:41–9.
22. Penna E, Orso F, Taverna D. miR-214 as a key hub that controls cancer networks: small player, multiple functions. J Invest Dermatol 2015;135: 960–9.
23. Zhang B, Liu XX, He JR, Zhou CX, Guo M, He M, et al. Pathologically decreased miR-26a antagonizes apoptosis and facilitates carcinogenesis by targeting MTDH and EZH2 in breast cancer. Carcinogenesis 2011; 32:2–9.
24. Sun YM, Lin KY, Chen YQ. Diverse functions of miR-125 family in different cell contexts. J Hematol Oncol 2013;6:6–14.
25. Sepe R, Formisano U, Federico A, Forzati F, Bastos AU, D'Angelo D, et al. CBX7 and HMGA1b proteins act in opposite way on the regulation of the SPP1 gene expression. Oncotarget 2015;6:2680–92.
26. O'Loghlen A, Muñoz-Cabello AM, Gaspar-Maia A, Wu HA, Banito A, Kunowska N, et al. MicroRNA regulation of Cbx7 mediates a switch of Polycomb orthologs during ESC differentiation. Cell Stem Cell 2012;10: 33–46.
27. Congrains A, Kamide K, Ohishi M, Rakugi H. ANRIL: molecular mechanisms and implications in human health. Int J Mol Sci 2013; 14:1278–92.
28. Chen D, Zhang Z, Mao C, Zhou Y, Yu L, Yin Y, et al. ANRIL inhibits p15 (INK4b) through the TGFβ1 signaling pathway in human esophageal squamous cell carcinoma. Cell Immunol 2014;289:91–6.
29. Hua L, Wang CY, Yao KH, Chen JT, Zhang JJ, Ma W. High expression of long non-coding RNA ANRIL is associated with poor prognosis in hepatocellular carcinoma. Int J Clin Exp Pathol 2015;8:3076–82.
30. Lin L, Gu ZT, Chen WH, Cao KJ. Increased expression of the long non-coding RNA ANRIL promotes lung cancer cell metastasis and correlates with poor prognosis. Diagn Pathol 2015;10:14–21.
31. Qiu JJ, Lin YY, Ding JX, Feng WW, Jin HY, Hua KQ. Long non-coding RNA ANRIL predicts poor prognosis and promotes invasion/metastasis in serous ovarian cancer. Int J Oncol 2015;46:2497–505.
32. Shinjo K, Yamashita Y, Yamamoto E, Akatsuka S, Uno N, Kamiya A, et al. Expression of chromobox homolog 7 (CBX7) is associated with poor prognosis in ovarian clear cell adenocarcinoma via TRAIL-induced apoptotic pathway regulation. Int J Cancer 2014;135:308–18.
33. Zheng X, Zhou J, Zhang B, Zhang J, Wilson J, Gu L, et al. Critical evaluation of Cbx7 downregulation in primary colon carcinomas and its clinical significance in Chinese patients. BMC Cancer 2015;15:145–55.
34. Karamitopoulou E, Pallante P, Zlobec I, Tornillo L, Carafa V, Schaffner T, et al. Loss of the CBX7 protein expression correlates with a more aggressive phenotype in pancreatic cancer. Eur J Cancer 2010;46:1438–44.
35. Pallante P, Terracciano L, Carafa V, Schneider S, Zlobec I, Lugli A, et al. The loss of the CBX7 gene expression represents an adverse prognostic marker for survival of colon carcinoma patients. Eur J Cancer 2010;46:2304–13.
36. Pallante P, Forzati F, Federico A, Arra C, Fusco A. Polycombprotein family member CBX7 plays a critical role in cancer progression. Am J Cancer Res 2015;5:1594–601.
37. Reijm EA, Timmermans AM, Look MP, Meijer-van Gelder ME, Stobbe CK, et al. High proteinexpression of EZH2 is related to unfavorable outcome to tamoxifen in metastatic breast cancer. Ann Oncol 2014;25:2185–90.
38. Wu J, Crowe DL. The histone methyltransferase EZH2 promotes mammary stem and luminal progenitor cell expansion, metastasis and inhibits estrogen receptor-positive cellular differentiation in a model of basal breast cancer. Oncol Rep 2015;34:455–60.

39. Chen S, Huang L, Sun K, Wu D, Li M, Li M, et al. Enhancer of zeste homolog 2 as an independent prognostic marker for cancer: a meta-analysis. PLoS One 2015;10:e0125480.
40. Morin RD, Johnson NA, Severson TM, Mungall AJ, An J, Goya R, et al. Somatic mutations altering EZH2 (Tyr641) in follicular and diffuse large B-cell lymphomas of germinal-center origin. Nat Genet 2010;42:181–5.
41. Sudo T, Utsunomiya T, Mimori K, Nagahara H, Ogawa K, Inoue H, et al. Clinicopathological significance of EZH2 mRNA expression in patients with hepatocellular carcinoma. Br J Cancer 2005;92:1754–8.
42. Völkel P, Dupret B, Le Bourhis X, Angrand PO. Diverse involvement of EZH2 in cancer epigenetics. Am J Transl Res 2015;7:175–93.
43. Koboldt DC, Fulton RS, McLellan MD, Schmidt H, Kalicki-Veizer J McMichael JF, et al. Comprehensive molecular portraits of human breast tumours. Nature 2012;490:61–70.
44. Derfoul A, Juan AH, Difilippantonio MJ, Palanisamy N, Ried T, Sartorelli V. Decreased microRNA-214 levels in breast cancer cells coincides with increased cell proliferation, invasion and accumulation of the Polycomb Ezh2 methyltransferase. Carcinogenesis 2011;32:1607–14.
45. Xiangxiang W, Xiaoyun D, Shengcan C, Haojun S, Haizhong J, Ying F, et al. The functional sites of miRNAs and lncRNAs in gastric carcinogenesis. Tumor Biol 2015;36:521–32.
46. Mansueto G, Forzati F, Ferraro A, Pallante P, Bianco M, Esposito F, et al. Identification of a new pathway for tumor progression: microRNA-181b up-regulation and CBX7 down-regulation by HMGA1 protein. Gene Cancer 2010;1:210–24.
47. Lee W, Teckie S, Wiesner T, Ran L, Prieto Granada CN, Lin M, et al. PRC2 is recurrently inactivated through EED or SUZ12 loss in malignant peripheral nerve sheath tumors. Nat Genet 2014;46:1227–32.
48. Fu LL, Tian M, Li X, Li JJ, Huang J, Ouyang L, et al. Inhibition of BET bromodomains as a therapeutic strategy for cancer drug discovery. Oncotarget 2015;6:5501–16.
49. Baude A, Lindroth AM, Plass C. PRC2 loss amplifies Ras signalingin cancer. Nat Genet 2014;46:1154–5.
50. De Raedt T, Beert E, Pasmant E, Luscan A, Brems H, Ortonne N, et al. PRC2 loss amplifies Ras-driven transcription and confers sensitivity to BRD4-based therapies. Nature 2014;514:247–51.